

# Electrospray Ionization Mass Spectrometry Reveals an Unexpected Coupling Product in the Copper-Promoted Synthesis of Pyrazoles

Jakub Hyvl,<sup>\*,†</sup> Divya Agrawal,<sup>†,§</sup> Radek Pohl,<sup>†</sup> Mamta Suri,<sup>‡</sup> Frank Glorius,<sup>‡</sup> and Detlef Schröder<sup>†,⊥</sup>

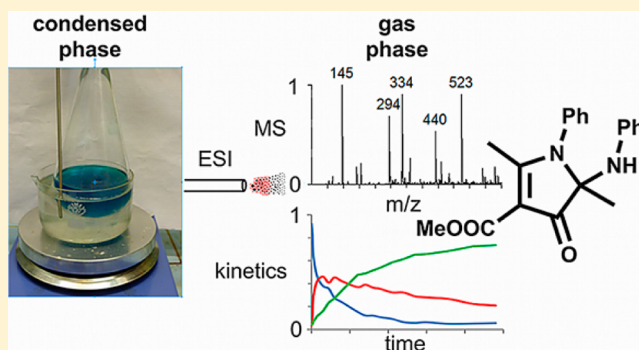
<sup>†</sup>Institute of Organic Chemistry and Biochemistry, Academy of Sciences of the Czech Republic, Flemingovo náměstí 2, 16610 Prague 6, Czech Republic

<sup>‡</sup>Organisch-Chemisches Institut, International NRW Graduate School of Chemistry, Westfälische Wilhelms-Universität Münster, Corrensstraße 40, 48149 Münster, Germany

<sup>§</sup>Organic Chemistry and Biochemistry, Leibniz-Institut für Molekulare Pharmakologie (FMP), Robert-Roessle-Straße 10, 13125 Berlin, Germany

## Supporting Information

**ABSTRACT:** The reaction mechanism of the intermolecular oxidative formation of pyrazole **2** via a C–C/N–N bond-formation cascade of the enaminone **1** is investigated by means of ESI-MS. No direct reaction intermediates are observed; however, the formation of an unexpected imidazolid-3-one derivative **X** is observed that involves an oxidative dimerization of **1** in the presence of dioxygen. The derivative **X** is isolated and characterized by means of multidimensional <sup>1</sup>H and <sup>13</sup>C NMR spectroscopy.



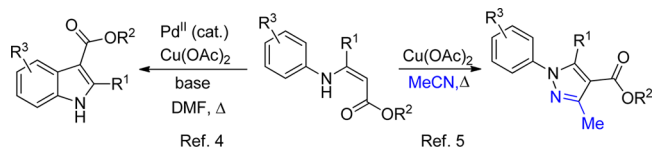
## INTRODUCTION

Copper catalysis not only belongs to the oldest themes in transition-metal catalysis but is also of current interest due to the manifold transformations comprising a broad spectrum of substrates and reactions,<sup>1</sup> combined with the environmental tolerance of copper and the reasonable price. An important group of such transformations are oxidative coupling reactions in which copper(II) serves as a mild oxidant, while the reoxidation  $\text{Cu}^{\text{I}} \rightarrow \text{Cu}^{\text{II}}$  can be accomplished by air as the terminal oxidant.<sup>2</sup> Often, the reactions appear to involve copper-peroxo species as unstable intermediates, but despite extensive efforts, the reaction mechanisms often remain elusive.<sup>3</sup>

Recently, an interesting example of this kind of reaction has been introduced, which can lead conveniently from easily prepared substrates to two important classes of heterocycles—indoles as well as pyrazoles—in a regioselective way, where the route to the desired target compound is determined by the choice of the catalyst system (Scheme 1).<sup>4,5</sup> Particularly attractive in terms of atom economy and the use of facile building blocks in general is the route to pyrazoles in which one molecule of the solvent ( $\text{CH}_3\text{CN}$ ) is incorporated into the product.<sup>6</sup> Moreover, this synthesis of pyrazoles has a conceptual difference from other routes, because the N–N bond is created in the decisive coupling step, whereas conventional pyrazole syntheses start from N–N precursors.

Regardless of the conceptual interest and the synthetic value of this transformation, the reaction mechanism has not been

## Scheme 1. Copper-Promoted Oxidative Cyclization of Enaminones Affords Indoles upon Coupled Pd/Cu Catalysis and Pyrazoles, While Using Only Cu and Acetonitrile As a Solvent



understood in detail. Here, we report a more detailed study of the route to pyrazoles by means of electrospray ionization mass spectrometry (ESI-MS),<sup>7</sup> which in recent years has been established as a valuable tool for the elucidation of reaction mechanisms and the identification of reactive intermediates, which is highly complementary to conventional methods in the condensed phase<sup>8,9</sup> and has successfully been applied in the elucidation of reaction mechanisms in copper catalysis.<sup>10</sup>

## EXPERIMENTAL METHODS

**Materials and Sample Preparation.** The synthesis and characterization of the starting enaminones has been described previously;<sup>4</sup> the preparation of the deuterium-labeled compounds is briefly reported in the Supporting Information. All other chemicals and solvents were purchased from Sigma-Aldrich and Penta Chemicals

Received: November 1, 2012

Published: January 29, 2013

and used as obtained without further purification. Unless otherwise mentioned, the condensed-phase reactions were performed by heating a solution of enaminone and  $\text{Cu}(\text{OAc})_2$  in  $\text{CH}_3\text{CN}$  to 110 °C in a round flask with a condenser and a Drierite guard tube. In given time intervals, small samples were taken, diluted with acetonitrile in a 1:100 ratio, and probed by means of ESI-MS. The final concentration of the sample after adjusting was about  $10^{-4}$  M.

**Instrumentation.** The studied solutions were examined with a Finnigan LCQ (ThermoFinnigan, San Jose, CA, USA) ion-trap mass spectrometer (IT-MS) equipped with an ESI source.<sup>11</sup> Nitrogen was used as the nebulizer gas, and the samples were introduced into the ESI source via a needle with a silica capillary (100  $\mu\text{m}$ ) at a flow rate of 2  $\mu\text{L min}^{-1}$ . The operating conditions were set as follows: source voltage 4 kV, capillary voltage -35 V, heated capillary temperature 100 °C, tube lens offset -35 V, sheath and auxiliary gas flow rate 10 arbitrary units. Under these conditions, the ionization in ESI is relatively soft, such that quasi-molecular ions as well as their aggregates with solvents can be observed.<sup>12,13</sup> For further characterization, dissociation of mass-selected ions was achieved by collisional activation via rf excitation using the helium buffer gas present in the ion trap as the collision partner. The collision energy was optimized for each experiment and is expressed in terms of the manufacturer's normalized collision energy (in %), where the range from 0 to 100% corresponds to a resonance excitations ac signal of 0–2.5 V (zero-to-peak) at the secular frequency of the ion of interest.<sup>14</sup> This energy depends on the  $m/z$  value of the parent ion and can be converted into an absolute scale by means of calibration.<sup>15</sup> Mass spectra were recorded from  $m/z$  50 to 2000 in positive-ion mode.

In order to support the elemental compositions assigned further below, additional exploratory experiments were performed with a SYNAPT G2 ion mobility instrument (Waters, Manchester, U.K.).<sup>16</sup> In brief, the instrument consists of an ESI source, from which the ions are extracted toward a quadrupole mass filter for the selection of parent ions; the ion-mobility mode was not used in these measurements. After extraction from the drift tube, the ions pass a transfer cell and enter the source region of a reflectron time-of-flight mass spectrometer, which continuously records mass spectra with a mass resolution ( $m/\Delta m$ ) of ca. 20 000. Accurate masses were determined via internal calibration with spiked reference compounds with known mass-to-charge ratios. The deviations less than 0.002 amu that were observed (see Table 1) fully support the assignments made on the basis of the IT-MS experiments.

NMR spectra were recorded on a Bruker Avance 500 (500 MHz for  $^1\text{H}$ , 125.7 MHz for  $^{13}\text{C}$ ) or Bruker Avance 400 (400 MHz for  $^1\text{H}$ , 100.6 MHz for  $^{13}\text{C}$ ) NMR spectrometer. Chemical shifts are given in  $\delta$ -scale as parts per million (ppm), and coupling constants ( $J$ ) are given in Hz. Infrared spectra were measured on a Bruker EQUINOX55 (IFS55) spectrometer in  $\text{CHCl}_3$  (cuvette width 0.118

mm). The HRMS spectrum of X was recorded on an LTQ Orbitrap XL in the FTMS +p ESI regime.

## RESULTS AND DISCUSSION

The strategy for investigation of the reaction mechanism in this paper is based on ESI-MS monitoring of the title reaction (Scheme 1). First, pure  $\text{Cu}(\text{OAc})_2$  in acetonitrile ( $10^{-4}$  M) and the pure substrate, i.e., methyl 3-(phenylamino)but-2-enoate (**1**) ( $6 \times 10^{-5}$  M), were characterized via ESI-MS, respectively. Second, a mixture of enaminone **1** and  $\text{Cu}(\text{OAc})_2$  was investigated at room temperature, and then the changes occurring upon heating were analyzed. In parallel, experiments with deuterium-labeled compounds as well as some homologues were carried out. Finally, a specific reaction intermediate, further below referred to as X, was isolated from the reaction mixture, fully characterized by usual spectroscopic methods, and then probed with regard to its role in the overall catalytic cycle.

We would like to mention at the very outset that the assignments of ions in ESI-MS are based on the ion masses, the isotope patterns, the additional isotope labeling experiments, and collision-induced dissociation experiments. Therefore, the formulas of the observed ions are not more than plausible suggestions, unless a complete spectroscopic characterization can be achieved, as in the case of X described below. Another important particularity of ESI-MS is that the different species present in solution may experience vastly different sampling probabilities in the electrospray ionization process. However, in studies of reactions occurring in the condensed phase with subsequent monitoring by ESI-MS, such discrimination effects can at least in part be compensated by following the changes of the mass spectra with reaction time in solution, which directly reflects the changes during chemical transformation. Discrimination factors need to be taken into account, which is quite straightforward, if the pure components are available as bulk substances (see below). Last but not least, it is pointed out that  $\text{CH}_3\text{CN}$  is used not only as solvent and reagent in the actual chemical transformation (at 110 °C) but in addition also for dilution of aliquot samples of the reaction mixtures before analysis via ESI-MS at room temperature. Accordingly,  $\text{CH}_3\text{CN}$  may either be chemically incorporated in the products via covalent bonds or act as a mere coordinative ligand of the metal center.

**Catalyst Solution and Enaminone Solution.** As a first reference point, a solution of anhydrous  $\text{Cu}(\text{OAc})_2$  in  $\text{CH}_3\text{CN}$  was analyzed via ESI-MS in the positive-ion mode (Figure 1a). Several adducts with  $\text{CH}_3\text{CN}$  were observed along with the reduction of  $\text{Cu}^{\text{II}}$  to  $\text{Cu}^{\text{I}}$  giving rise to  $[\text{Cu}(\text{CH}_3\text{CN})_2]^+$  as the major signal at  $m/z$  145. Note that all  $m/z$  values given below refer to the leading isotopes, i.e.,  $^1\text{H}$ ,  $^{12}\text{C}$ ,  $^{14}\text{N}$ ,  $^{16}\text{O}$ , and  $^{63}\text{Cu}$ , and that the assignment of elemental compositions was substantiated by high-resolution mass measurements (see the Supporting Information). As far as the reduction from  $\text{Cu}^{\text{II}}$  to  $\text{Cu}^{\text{I}}$  is concerned in the binary  $\text{Cu}(\text{OAc})_2/\text{CH}_3\text{CN}$  system, it occurs during the electrospray process as demonstrated elsewhere,<sup>15a,17</sup> but in the course of the title reaction, reduction to the copper(I) manifold also occurs in solution.<sup>18</sup>

As a second point of reference, a solution of enaminone **1** in  $\text{CH}_3\text{CN}$  was subjected to ESI-MS analysis in the positive-ion mode. Under soft ionization conditions, the most abundant signal is observed at  $m/z$  192, which corresponds to the protonated enaminone **1** (Figure 1b).

**Table 1.** Measured ( $m_{\text{exp}}$ ) and Calculated ( $m_{\text{calc}}$ ) Masses of Selected Ions Discussed in the Text As Derived from High-Resolution Mass Determination<sup>a</sup>

	nominal mass	$m_{\text{exp}}$	$m_{\text{calc}}$	$\Delta m^b$
$[\text{1H}]^+$	192	192.1021	192.1024	-0.3
$[\text{2H}]^+$	231	231.1138	231.1133	0.5
$[(\text{1-H})\text{Cu}(\text{CH}_3\text{CN})]^+$	294 <sup>c</sup>	294.0442	294.0429	1.3
$[(\text{1})\text{Cu}(\text{CH}_3\text{CN})]^+$	295 <sup>d</sup>	295.0520	295.0508	1.2
$[(\text{2})\text{Cu}(\text{CH}_3\text{CN})]^+$	334	334.0628	334.0617	1.1
$[(\text{X})\text{Cu}(\text{CH}_3\text{CN})]^+$	440	440.1037	440.1035	0.2
$[(\text{1})\text{Cu}(\text{2})]^+$	484	484.1295	484.1297	-0.2
$[(\text{2})_2\text{Cu}]^+$	523	523.1398	523.1406	-0.8
$[(\text{X})\text{Cu}(\text{2})]^+$	629	629.1816	629.1825	-0.9
$[(\text{X})_2\text{Cu}]^+$	735	735.2251	735.2244	0.7

<sup>a</sup>Monoisotopic masses for the leading isotopes. <sup>b</sup> $\Delta m = m_{\text{exp}} - m_{\text{calc}}$  in milli-amu. <sup>c</sup>Prevailing signal in this mass region before heating. <sup>d</sup>Prevailing signal in this mass region after heating **1** to 110 °C.

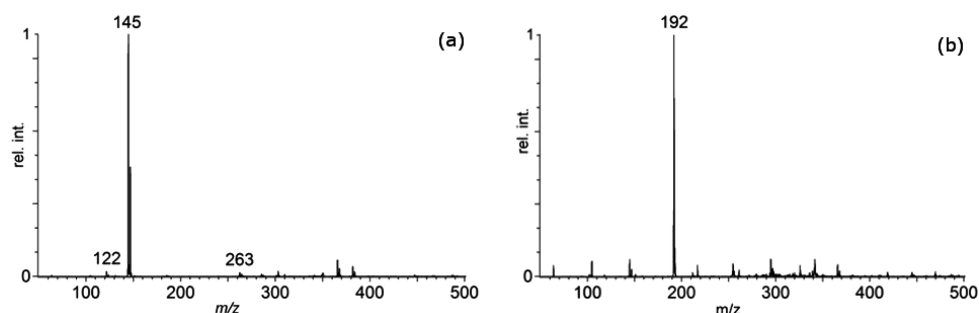


Figure 1. ESI-MS of (a)  $\text{Cu}(\text{OAc})_2$  and (b) the enaminone **1** in pure  $\text{CH}_3\text{CN}$  under soft ionization conditions.

### Catalyst and Enaminone Solution without Heating.

Next, 1.5 equiv of  $\text{Cu}(\text{OAc})_2$  was added to a 0.013 M acetonitrile solution of enaminone **1** in the presence of air, and the reaction mixture was stirred at room temperature. At regular intervals of time, aliquots from the reaction mixture were 100-times diluted with  $\text{CH}_3\text{CN}$  and analyzed by ESI-MS. The obtained spectra did not show any major changes at room temperature even after 8 h of stirring (Figure 2). The major

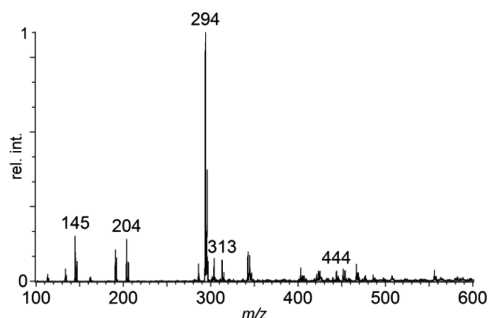


Figure 2. ESI-MS of a solution of the enaminone **1** (0.013 M) and  $\text{Cu}(\text{OAc})_2$  (0.019 M) in  $\text{CH}_3\text{CN}$  in the positive-ion mode.

signal at  $m/z$  294 in the spectrum can be attributed to the complex of the deprotonated substrate with copper(II) and one additional acetonitrile ligand, i.e.,  $[(\text{CH}_3\text{CN})\text{Cu}(\mathbf{1}-\text{H})]^+$ . Other peaks at  $m/z$  204, 313, and 444 are assigned to  $[(\text{CH}_3\text{CN})_2\text{Cu}(\text{OAc})]^+$ ,  $[(\mathbf{1})\text{Cu}(\text{OAc})]^+$ , and  $[(\mathbf{1})\text{Cu}(\mathbf{1}-\text{H})]^+$ , respectively. Hence, we conclude that in acetonitrile solution the  $\text{Cu}(\text{OAc})_2$  catalyst forms a complex with the reactant in which the deprotonated unit ( $\mathbf{1}-\text{H}$ ) replaces an acetate ligand.

While we have not performed a specific labeling experiment, the mere structure of the reactant **1** implies that the NH proton is abstracted, leading to a chelating ligand in analogy to the common acetylacetonate (acac) system. Further support is provided by a collision-induced dissociation (CID) experiment with mass-selected ion  $[(\mathbf{1})\text{Cu}(\text{OAc})]^+$  ( $m/z$  313), which leads to loss of acetic acid followed by uptake of a acetonitrile ligand from the background solvent diffusing into the IT-MS from the source region and finally resulting in  $[(\text{CH}_3\text{CN})\text{Cu}(\mathbf{1}-\text{H})]^+$  ( $m/z$  294).<sup>19</sup> Hence the counterion on copper serves as the base abstracting the proton. The finding that already acetate can provide the NH-deprotonation of the enamine can be attributed to the favorable coordination of the metal by the

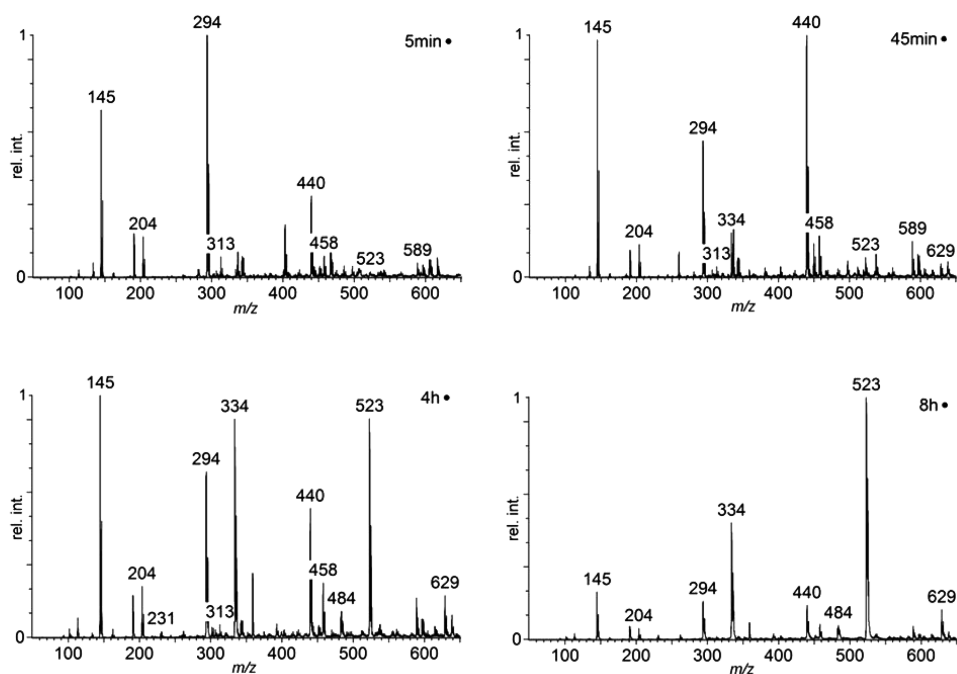


Figure 3. Positive-ion ESI-MS of a solution of the enaminone **1** (0.013 M) and  $\text{Cu}(\text{OAc})_2$  (0.019 M) in  $\text{CH}_3\text{CN}$  in the positive-ion mode upon heating to 110 °C for various times ranging from 5 min to 8 h.

chelating ligand. At low collision energies, CID experiments with the mass-selected ion  $[(\text{CH}_3\text{CN})\text{Cu}(\text{1-H})]^+$  show the loss of  $\text{CH}_3\text{CN}$  as exclusive fragmentation. Also at elevated collision energies there are no indications for the occurrence of C–N coupling.<sup>20</sup> Specifically, no fragments are observed that can be attributed to the pyrazole product, e.g., the radical cation  $2^{+\bullet}$  ( $m/z$  230) or the protonated form  $[2 + \text{H}]^+$  ( $m/z$  231). Thus, mere energizing of the reactant complex  $[(\text{CH}_3\text{CN})\text{Cu}(\text{1-H})]^+$  does not trigger bond formation, suggesting that the process in solution requires additional factors, i.e., the presence of molecular oxygen as well as elevated temperatures.

**Catalyst and Enaminone Solution with Heating.** Next, the above solution was stirred at 110 °C with a  $\text{CaCl}_2$  guard tube allowing open access to air. At regular intervals of time, aliquots were diluted 100 times with  $\text{CH}_3\text{CN}$  and analyzed by ESI-MS.

Figure 3 shows a series of ESI mass spectra obtained upon heating the reaction mixture for various intervals of time. All of these spectra show the presence of the  $\text{Cu}^{\text{I}}$  species  $[(\text{CH}_3\text{CN})_2\text{Cu}]^+$  at  $m/z$  145 along with the corresponding  $\text{Cu}^{\text{II}}$  ions  $[(\text{CH}_3\text{CN})_2\text{Cu}(\text{OAc})]^+$  ( $m/z$  204) and  $[(\text{CH}_3\text{CN})\text{Cu}(\text{1-H})]^+$  ( $m/z$  294). In addition, a signal at  $m/z$  313 assigned to  $[(\text{1})\text{Cu}(\text{OAc})]^+$  is present in small abundance and disappears completely after 8 h of stirring. As a reflection of the progress of the reaction in the condensed phase, ions at  $m/z$  231, 334, and 523 increase gradually with time, which are ascribed to ions due to the reaction product formed according to Scheme 1, i.e., methyl 3,5-dimethyl-1-phenyl-1H-pyrazole-4-carboxylate (**2**). These ions are accordingly ascribed to  $[2\text{H}]^+$  ( $m/z$  231),  $[(2)\text{Cu}(\text{CH}_3\text{CN})]^+$  ( $m/z$  334), and  $[\text{Cu}(2)_2]^+$  ( $m/z$  523), respectively. Likewise, cations at  $m/z$  483 and 484 are accordingly attributed to copper complexes consisting of the enaminone **1** and the pyrazole **2**, i.e.,  $[(2)\text{Cu}(\text{1-H})]^+$  and  $[(\text{1})\text{Cu}(2)]^+$ , respectively.

The abundances of ions at  $m/z$  440, 458, 589, 597, and 629 become relatively large after 45 min of stirring, suggesting their presence as important intermediates in the reaction mixture. To assign these signals (shown in Figure 3), collision-induced dissociation experiments, kinetic studies, and reactions with labeled compounds, which are discussed below, were performed. These experiments revealed that the mentioned peaks contain a new component **X** with a nominal mass of 336 g/mol; from the differences in the HR measurement (Table 1), we derive  $m_{\text{exp}} = 336.1476 \text{ g mol}^{-1}$ , for which the nearest hit with  $m_{\text{calc}} = 336.1474 \text{ g mol}^{-1}$  corresponds to the formula  $\text{C}_{20}\text{H}_{20}\text{N}_2\text{O}_3$ . Other signals related with compound **X** in the spectra are  $[(\text{X})\text{Cu}(\text{CH}_3\text{CN})]^+$  ( $m/z$  440),  $[\text{Cu}(\text{X})(\text{OAc})]^+$  ( $m/z$  458),  $[(\text{X})\text{Cu}(\text{1-H})]^+$  ( $m/z$  589), and  $[(\text{X})\text{Cu}(2)]^+$  ( $m/z$  629). The structure of compound **X** is discussed in more detail further below in the text.

**Reaction Kinetics Followed via ESI-MS.** Next, the various ion signals in ESI-MS were followed as a function of reaction time in solution, which provides insight into the reaction kinetics,<sup>21</sup> although the concentrations in solution and the ion abundances in the gas phase may not show a 1:1 correlation.<sup>22</sup> Actual ratios of ion abundances of observed species is discussed in detail in the section Discrimination in ESI Sampling of Reaction Partners. Figure 4 shows the time behavior of the most significant components for the intermolecular oxidative formation of the pyrazole **2** via the C–C/N–N bond-formation cascade of the enaminone **1**. To this end, we consider the sum of the abundances of  $[\text{Cu}(\text{1})(\text{CH}_3\text{CN})]^+$ ,  $[\text{Cu}(\text{1})(2)]^+$ ,  $[\text{Cu}(\text{1})_2]^+$ , and  $[\text{Cu}(\text{1})(\text{X})]^+$  for the starting enaminone **1**,

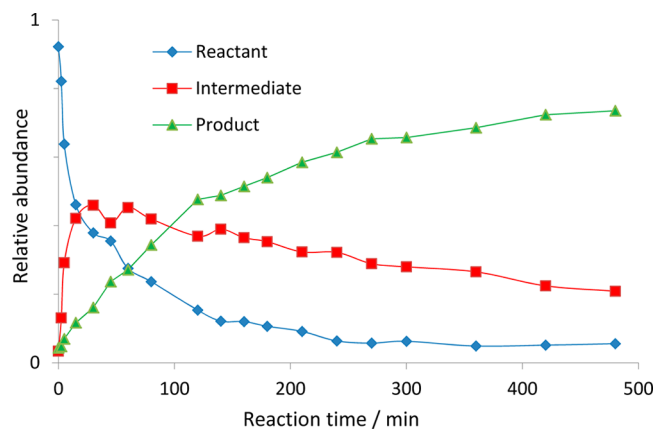


**Figure 4.** Dependence of the relative intensities of the main components from the time of heating in solution to 110 °C as monitored via ESI-MS in the positive-ion mode. For the sake of clarity, the individual ions are not shown, but the sum of ions containing the reactant **1**, the product **2**, and the potential intermediate **X**, respectively, normalized to  $\sum = 1$  is shown. We note in passing that in this particular experiment the labeled reactant **1c** (with a  $\text{COOCD}_3$  group) was used.

the sum of the abundances of  $[\text{Cu}(2)(\text{CH}_3\text{CN})]^+$ ,  $[\text{Cu}(2)_2]^+$ ,  $[\text{Cu}(2)(\text{X})]^+$ , and  $[\text{Cu}(\text{1})(2)]^+$  is considered for the pyrazole **2**, and  $[\text{Cu}(\text{X})(\text{CH}_3\text{CN})]^+$ ,  $[\text{Cu}(\text{1})(\text{X})]^+$ ,  $[\text{Cu}(\text{X})_2]^+$ , and  $[\text{Cu}(2)(\text{X})]^+$  are taken for compound **X**. The enaminone **1** and the pyrazole **2** have typical kinetic profiles expected for starting materials and products of a chemical reaction. The time dependence of the ions associated with compound **X** coincides with the behavior expected for a reaction intermediate with a strong increase in the first 15 min, which is faster than that of the product complexes, while at longer reaction times the signals of **X** decrease significantly.

In this context, we also addressed the stoichiometric oxidation of the substrate by  $\text{Cu}(\text{OAc})_2$  under anaerobic conditions. Formally, the conversion  $1 + \text{CH}_3\text{CN} \rightarrow 2$  releases two hydrogen atoms, which need to be taken up by an oxidant to provide the required thermochemical driving force. In the preparative procedure of the title reaction, the terminal oxidant is aerobic oxygen. However,  $\text{Cu}(\text{OAc})_2$  itself can also serve as oxidant. If such a redox reaction takes place, pyrazole formation should already be observed in the absence of oxygen, and in the case of a reduction from  $\text{Cu}^{\text{II}}$  to  $\text{Cu}^{\text{I}}$ , no more than 0.5 equiv of **2** could be formed relative to  $\text{Cu}(\text{OAc})_2$ , whereas reduction to  $\text{Cu}^0$  would result in a 1:1 stoichiometry under anaerobic conditions. To this end, the title reaction was performed under argon with different amounts of  $\text{Cu}(\text{OAc})_2$ , followed by conventional workup and analysis via gas chromatography (GC; with dimethyl terephthalate added after workup as an internal standard). The results shown in Figure 5 indicate that at least partially  $\text{Cu}^{\text{II}}$  can indeed act as a two-electron oxidant, as for low ratios between  $\text{Cu}(\text{OAc})_2$  and **1**, the yields significantly exceed the maximal yield expected for the  $\text{Cu}^{\text{II}}/\text{Cu}^{\text{I}}$  redox couple. The yields of the reactions with more than 1 equiv of  $\text{Cu}(\text{OAc})_2$  were also influenced by its limited solubility in  $\text{CH}_3\text{CN}$ , leading to lower conversions than expected. We further note in passing that the ESI measurements of the reaction mixtures from anaerobic conditions show negligible signals due to **X**, while those of **1** as well as **2** correspond to those under aerobic conditions.

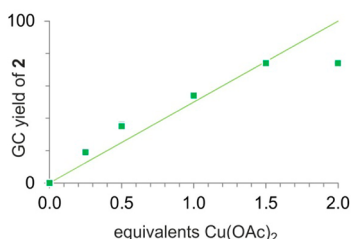


**Figure 5.** Dependence of yield of the pyrazole **2** (determined via gas chromatography with internal standard) on the amount of  $\text{Cu}(\text{OAc})_2$  under anaerobic conditions. The solid diagonal represents the maximal theoretical yield for copper(II) acting as a single-electron oxidant.

**Heating Followed by Dilution with  $\text{CD}_3\text{CN}$ .** In order to confirm the assignments of various signals, the reactant solution after 8 h of stirring at  $110^\circ\text{C}$  was diluted with  $\text{CD}_3\text{CN}$  (instead of  $\text{CH}_3\text{CN}$ ) and then analyzed using ESI-MS (Figure 6). In the case of noncovalent complexes, a rapid exchange of  $\text{CH}_3\text{CN}$  by  $\text{CD}_3\text{CN}$  is expected to occur, which would be manifested by the corresponding mass shifts ( $\Delta m = +3$  per acetonitrile

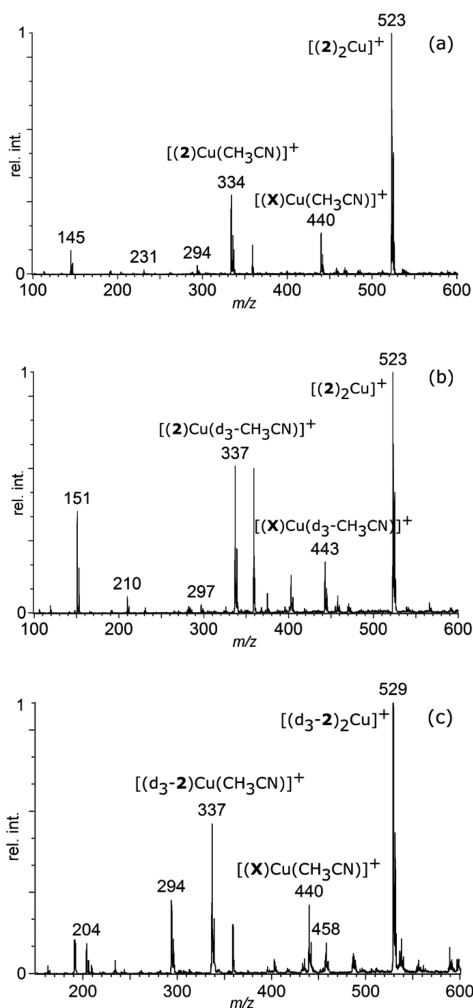


**Figure 6.** (a) Positive-ion ESI-MS spectra obtained with  $\text{CH}_3\text{CN}$  followed by 1:100 dilution with  $\text{CH}_3\text{CN}$  and (b) the corresponding experiment after 1:100 dilution with  $\text{CD}_3\text{CN}$  prior to the sampling. (c) Positive-ion ESI-MS of the solution of 0.026 mmol of enaminone **1** and 1.5 equiv of  $\text{Cu}(\text{OAc})_2$  in  $\text{CD}_3\text{CN}$  (2 mL) after 5 h heating to  $110^\circ\text{C}$  and 1:100 dilution with  $\text{CH}_3\text{CN}$  prior to sampling.

ligand). For the signal at  $m/z$  334, a shift by  $\Delta m = +3$  is indeed observed upon dilution with  $\text{CD}_3\text{CN}$ , thus confirming the presence of one free acetonitrile ligand in the ion, which is fully consistent with the assignment as  $[(2)\text{Cu}(\text{CH}_3\text{CN})]^+$ , in which the  $\text{CH}_3\text{CN}$  incorporated into the product **2** stems from the reactive solution and not from dilution and is thus unlabeled. However, the signal at  $m/z$  523 does not shift, indicating the absence of any coordinated acetonitrile ligand, as expected for the product complex  $[\text{Cu}(2)_2]^+$ , in which both acetonitrile units are embedded covalently. A shift of  $\Delta m = +3$  for the ion at  $m/z$  440 further confirms the presence of one noncovalently bound acetonitrile ligand, as suggested in the assigned formula  $[(X)\text{Cu}(\text{CH}_3\text{CN})]^+$ .

**$\text{CD}_3\text{CN}$  As Solvent in the Reaction.** In complement to the previous labeling study, next deuterated  $\text{CD}_3\text{CN}$  was used as the solvent in the reaction, whereas the dilution prior to ESI-MS was done with unlabeled  $\text{CH}_3\text{CN}$ . To this end, a solution of 0.024 mmol of the enaminone **1** and 1.5 equiv of  $\text{Cu}(\text{OAc})_2$  in  $\text{CD}_3\text{CN}$  (2 mL) was stirred at  $110^\circ\text{C}$  in a flask with water condenser, a  $\text{CaCl}_2$  guard tube, and open access to air. At regular intervals of time, aliquots were taken from the reaction mixture and after 100 times diluting with  $\text{CH}_3\text{CN}$  were subjected to ESI-MS analysis in the positive mode. The use of  $\text{CH}_3\text{CN}$  as the solvent in the reaction results in an intermolecular oxidative formation of pyrazole via a C–C/N–N bond-formation cascade (Scheme 1). The use of  $\text{CD}_3\text{CN}$  as the solvent in the reaction itself would thus lead to a shift by  $\Delta m = +3$  for all species bearing the covalently embedded  $\text{CH}_3\text{CN}$ , whereas those with a noncovalent acetonitrile ligand should not show a mass shift due to the subsequent dilution with  $\text{CH}_3\text{CN}$ . In the corresponding spectrum obtained after 5 h of stirring (Figure 6), the signals at  $m/z$  334 and 629 show the expected shifts by  $\Delta m = +3$ , indicating the presence of one covalently linked nitrile, and likewise the signal at  $m/z$  523 shifts by  $+6$  mass units, confirming the presence of two covalently linked nitrile moieties. This experiment further demonstrates that the ions at  $m/z$  294, 440, and 458 do not bear covalently bound  $\text{CH}_3\text{CN}$  because no mass shifts occur when  $\text{CD}_3\text{CN}$  is used as a reaction solvent, but the subsequent dilution applies  $\text{CH}_3\text{CN}$ .

**Reactions of Labeled Starting Material.** To find out more information about the component X, reactions with labeled compounds were performed. First, methyl 3-(*p*-tolylamino)but-2-enoate (**1b**) was prepared and subjected to the reaction at the same reaction conditions as above (i.e., 0.024 mmol of **1b**, 1.5 equiv of  $\text{Cu}(\text{OAc})_2$ , 2 mL of  $\text{CH}_3\text{CN}$ ,  $110^\circ\text{C}$ ,  $\text{CaCl}_2$  guard tube, reaction time 8 h). At regular intervals of time aliquots were taken from the reaction mixture and after 100 times diluting with  $\text{CH}_3\text{CN}$  were subjected to ESI-MS analysis in the positive mode. Figure 7a shows that the peak obtained at  $m/z$  440 in the case of reactant **1** shifts by  $\Delta m = +28$  to  $m/z$  468 for **1b**, suggesting the presence of two covalently linked aniline moieties in X.

Second, [ $\text{D}_3$ -methyl] 3-(*p*-phenylamino)but-2-enoate (**1c**) was prepared by selective deuteration, and 0.026 mmol of this compound was subjected to the same reaction conditions and measurements as described in the previous paragraph. Figure 7b shows that the peak at  $m/z$  440 is shifted by  $\Delta m = +3$  mass units, indicating the presence of one carboxymethyl group in the unknown compound X.

Further, an analogous experiment with deuterated acetate, i.e.,  $(\text{CD}_3\text{COO})_2\text{Cu}$ , under identical conditions gave no significant mass shifts for the ions related with compound X,

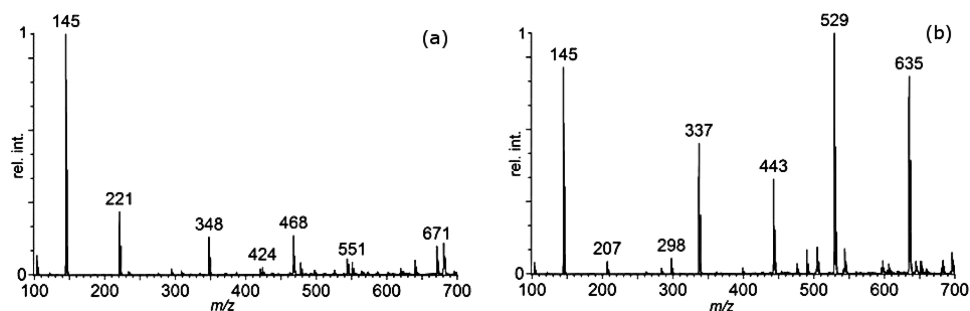


**Figure 7.** Positive-ion ESI-MS of the solutions of the enaminones (a) **1b** and (b) **1c**, respectively, and 1.5 equiv of  $\text{Cu}(\text{OAc})_2$  in  $\text{CH}_3\text{CN}$  (2 mL) at  $110^\circ\text{C}$  after 4 h stirring.

**Table 2.** Ions Observed upon CID of Mass-Selected  $m/z$  399, the Associated Mass Differences and Ion Abundances, As Well As the High-Resolution Data of the Measured ( $m_{\text{exp}}$ ) and Calculated ( $m_{\text{calc}}$ ) Masses<sup>a,b</sup>

	nominal mass	$I_{\text{LE}}^c$	$I_{\text{HE}}^d$	$\Delta m_{\text{frag}}^e$	$m_{\text{exp}}$	$m_{\text{calc}}$	$\Delta m^f$
$[(\text{X})\text{Cu}]^+$	399	100	2		399.0764	399.0770	-0.6
- $\text{CH}_3\text{OH}$	367	2	2	-32	367.0501	367.0508	-0.7
- $\text{C}_6\text{H}_5\text{NH}^*$	307	7	100	-92	307.0269	307.0270	-0.1
- $\text{C}_6\text{H}_5\text{NH}_2$	306	4	40	-93	306.0191	306.0195	0.4
- $\text{C}_6\text{H}_5\text{NHCu}$	244		8	-155	244.0985	244.0974	1.1
- $(\text{C}_6\text{H}_5\text{NHCu} + \text{CH}_3\text{OH})$	212	1	55	-187	212.0718	212.0711	0.7

<sup>a</sup>For generation of  $[(\text{X})\text{Cu}]^+$ , the source conditions need to be made harsher, in order to induce fragmentation of the direct precursor  $[(\text{X})\text{Cu}(\text{CH}_3\text{CN})]^+$ . <sup>b</sup>Monoisotopic masses for the leading isotopes. <sup>c</sup>Ion abundance (base peak = 100) at low-energy CID; 10 V excitation voltage in SYNAPT G2. <sup>d</sup>Ion abundance (base peak = 100) at high-energy CID; 30 V excitation voltage in SYNAPT G2. <sup>e</sup>Mass differences corresponding to the neutral species lost. <sup>f</sup>Difference of HR measurements:  $\Delta m = m_{\text{exp}} - m_{\text{calc}}$  in milli-amu.

which hence does not contain an acetate moiety from the copper(II) acetate catalyst.

**CID of Mass-Selected  $m/z$  399 and 440.** In order to achieve further insight into the structure of **X**, high-resolution CID mass spectra of the ions  $[(\text{X})\text{Cu}]^+$  ( $m/z$  399) and  $[(\text{X})\text{Cu}(\text{CH}_3\text{CN})]^+$  ( $m/z$  440) were recorded. While the latter ion shows predominant loss of  $\text{CH}_3\text{CN}$ , the fragmentation of  $[(\text{X})\text{Cu}]^+$  is more insightful (Table 2). As structurally indicative fragments we observed (i) a loss of methanol ( $\Delta m = -32$ ), suggesting the persistence of one carboxymethyl group from the reactant **1**, and (ii) loss of an aniliny radical ( $\Delta m = -92$ ) as well as aniline ( $\Delta m = -93$ ), indicating the presence of at least one of the heterosubstituents; the other fragments listed can be understood as consecutive reactions of these primary processes. Furthermore, the occurrence of bond homolysis (*i.e.*, loss of  $\text{C}_6\text{H}_5\text{NH}^*$ ) strongly suggests that **X** is a covalent compound, rather than a loose complex of two (or more) subunits.

**Summary of the Mass Spectrometric Evidence about Compound X.** The monitoring of the reaction kinetics using ESI-MS (Figure 4) suggests compound **X** as a possible intermediate in the title reaction, and therefore its identity may help to understand the course of the reaction. To this end, let us reconcile the information achieved so far about **X**, for which we have established the elemental composition  $\text{C}_{20}\text{H}_{20}\text{N}_2\text{O}_3$  by means of high-resolution mass measurements. At first, the experiments with labeled  $\text{CH}_3\text{CN}$  and acetate, respectively, reveal that these compounds are not incorporated into **X**, and hence the only source of carbon is the reactant molecule **1**. Formally, the formula of **X** corresponds to a dimerization of **1** after loss of " $\text{C}_2\text{H}_6\text{O}$ ". The experiment with the  $\text{D}_3$ -labeled enamine **1c** as well as the CID data indicates the presence of one carboxymethyl group in **X**. Further, the experiment with the derivative **1b** as well as the CID data implies the incorporation of two aniliny groups into **X**, of

which at least one appears to still bear the NH proton (the other is shown gray). These various pieces of information are collected in Scheme 2. At this point, however, the mass

**Scheme 2.** Structural Elements of Compound **X** As Deduced from the ESI-MS Data



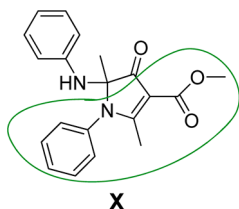
spectrometric data cannot provide more information about the structure of the core of compound **X**, and accordingly there is a need to achieve independent structural insight.

**Isolation of Compound X.** From the kinetic profile of compound **X** upon ESI-MS monitoring (Figure 4) it can be estimated that the concentration of **X** in the reaction mixture reaches a maximum at about 15 min of reaction time. Moreover, at least in the mass spectrometric monitoring the ions containing **X** constitute a considerable share of the total ion current at short reaction times. Further, the CID experiments indicate that **X** is not a loosely bound aggregate but a covalently bound species. Accordingly, we attempted to isolate compound **X** from the reaction mixture.

To this end, the reaction was scaled up and 1.0 mmol of enaminone **1** was treated with 1.5 equiv of  $\text{Cu}(\text{OAc})_2$  in 76 mL of  $\text{CH}_3\text{CN}$ . The reaction was stirred at  $110^\circ\text{C}$  for 15 min in a reaction flask with a water condenser, a  $\text{CaCl}_2$  guard tube, and open access to air. After this period, the mixture was cooled rapidly, EDTA was added to remove  $\text{Cu}(\text{OAc})_2$  from the reaction mixture, and isolation of compound **X** was carried out by column chromatography. Upon elution with ethyl acetate over silica gel, compound **X** (5 mg) was isolated in 3% yield

from the reaction mixture also containing starting enaminone **1a** and pyrazole **2**. Characterization was performed by means of multidimensional  $^1\text{H}$  and  $^{13}\text{C}$  NMR spectroscopy. On the basis of a structurally similar compound as well as the NMR data obtained, the molecular structure shown in Scheme 3 is

### Scheme 3. Proposed Structure of X Based on Multidimensional NMR Spectroscopy



suggested, which is consistent with all information available from NMR (see the Supporting Information) and agrees with the structural implications of the ESI-MS data (Scheme 2).

Specifically, compound **X** has an imidazolid-3-one skeleton, and the lower part of the molecule (encircled in green) resembles one equivalent of the starting material **1**. Due to the lack of other carbon sources in the reaction mixture, also the top hemisphere of compound **X** must stem from **1**, but the route toward structure **X** is not obvious upon first sight.

#### Role of Compound X As a Reaction Intermediate.

Once having isolated the pure compound, we can also return to the title reaction and prove or disprove the hypothesis that compound **X** is an intermediate of the intermolecular oxidative formation of the pyrazole **2** via a C–C/N–N bond-formation cascade of the enaminone **1**. To this end, a solution of compound **X** and  $\text{Cu}(\text{OAc})_2$  in  $\text{CH}_3\text{CN}$  was heated to  $120\text{ }^\circ\text{C}$ . Unfortunately, the sample of **X** obtained from chromatography is contaminated by traces of sodium, such that the ESI mass spectrum obtained immediately after heating is dominated by peaks due to  $[(\text{X})\text{Na}]^+$  ( $m/z$  359) and  $[(\text{X})_2\text{Na}]^+$  ( $m/z$  695); nevertheless, the complex  $[(\text{X})\text{Cu}(\text{CH}_3\text{CN})]^+$  ( $m/z$  440) is clearly visible in the mass spectrum (Figure 8a). If compound **X** was an intermediate of the title reaction shown in Scheme 2, the formation of complexes due to the product **2** should be observed at extended reaction times. After 30 min of heating at  $120\text{ }^\circ\text{C}$ , no indication for the formation of the product **2** was obtained and instead peaks with higher  $m/z$  values appeared (735, 809, 1030, and 1056), indicating the occurrence of some side reactions (Figure 8b).

A possible mechanism for the formation of **X** could involve the oxidation at the  $\alpha$ -position followed by the addition of a second molecule of enaminone **1**, hydrolysis, and decarbox-

ylation (Scheme 4). In this context, it is mentioned that the structure of the potential reaction intermediate and of the actual compound **X** isolated after workup do not need to be identical. Nonetheless, the CID experiments of  $[(\text{X})\text{Cu}(\text{CH}_3\text{CN})]^+$  ( $m/z$  440) obtained from the solution of the isolated compound **X** with copper(II) acetate are identical with spectra obtained directly from the reaction mixture.

Strong support for this suggestion comes from an experiment performed with  $^{18}\text{O}_2$  instead of normal air in which the signal at  $m/z$  440 due to the complex  $[(\text{X})\text{Cu}(\text{CH}_3\text{CN})]^+$  (trace (a) in Figure 9) is shifted to  $m/z$  442 ( $\Delta m = 2$ , trace (b)), precisely as expected for the incorporation of a single O atom from dioxygen in compound **X**. Some amount of  $[^{16}\text{O}]\text{-X}$  in trace (b) as apparent by the remainder at  $m/z$  440 is assigned to other sources of oxygen atoms, such as moisture or a small amount of leaking-in air.

As demonstrated above, the time dependence of the abundance of **X** suggests its involvement as a reaction intermediate (Figure 4), whereas the corresponding control experiment reveals that **X** does not lead to the product (Figure 8). Hence, compound **X** appears to be a mere side product of the reaction, whereas the product of an oxidative dimerization is formed at a larger rate in early stages of the reaction, when the concentration of the starting material is still large. However, we speculated that compound **X** also might act as a cocatalyst in the pyrazole formation. To this end, we added **X** to the reaction mixture and indeed could observe moderate acceleration of the product formation at early stages of the reaction (Figure 10).

#### Discrimination in ESI Sampling of Reaction Partners.

Last but not least, there remains a question of why monitoring the title reaction with ESI-MS shows pronounced participation of **X**, whereas the isolated yield was only 3% and the control experiment (Figure 8) rules out the suggestion of **X** as a reaction intermediate. This result indicates that the ESI-MS monitoring must somehow be biased in quantitative terms. In fact, it is well-known that ionization efficiencies may largely differ for different compounds in ESI-MS. In the present case, the copper-ion affinities are obviously decisive. In order to address this particular aspect, we prepared a 1:1:1 mixture of **1**, **2**, and **X** and added either 1 or 3 equiv of  $\text{Cu}(\text{OAc})_2$ . In the resulting spectra (Figure 11), the expected signals due to  $[(2)\text{Cu}(\text{CH}_3\text{CN})]^+$  ( $m/z$  334),  $[(\text{X})\text{Cu}(\text{CH}_3\text{CN})]^+$  ( $m/z$  440),  $[(2)_2\text{Cu}]^+$  ( $m/z$  523), and  $[(\text{X})\text{Cu}(2)]^+$  ( $m/z$  629) are clearly observed, although not in a 1:1 ratio. Detailed inspection of the low-mass region reveals small contributions of  $[(1\text{-H})\text{Cu}(\text{CH}_3\text{CN})]^+$  ( $m/z$  294) and  $[(1)\text{Cu}(\text{CH}_3\text{CN})]^+$  ( $m/z$  295), as well as  $[(1)\text{Cu}(2)]^+$  ( $m/z$  484), but these are about 2 orders of magnitude less abundant than the signals due to copper complexes of the product **2** and species **X**. Hence, the

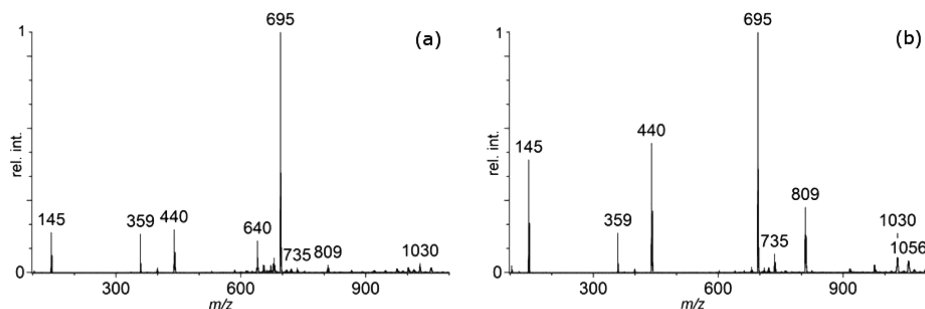
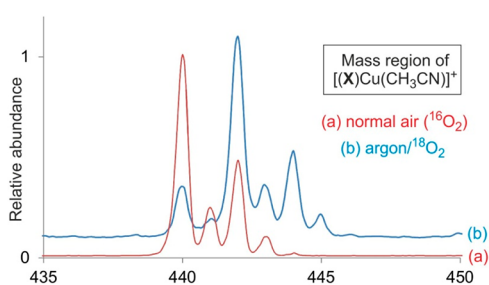
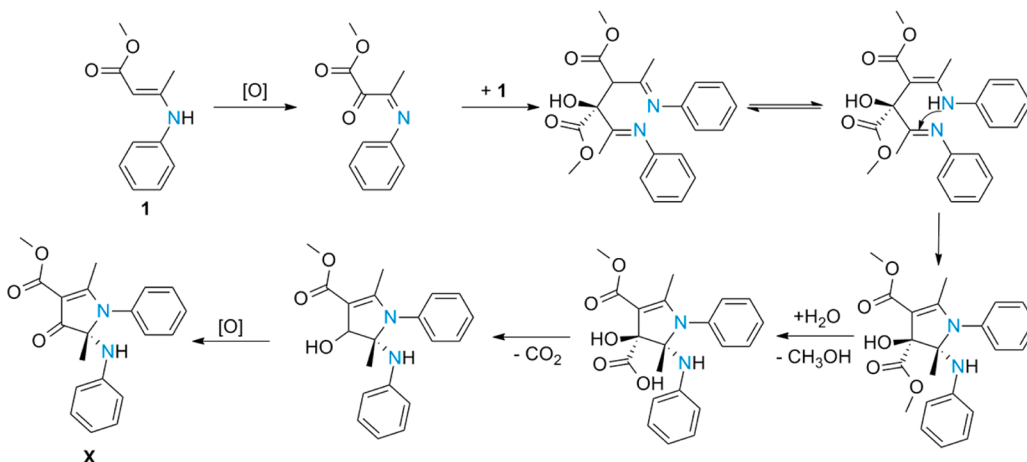
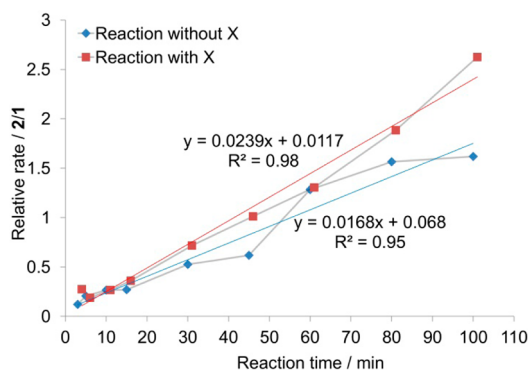


Figure 8. Reaction of compound **X** and  $\text{Cu}(\text{OAc})_2$  in  $\text{CH}_3\text{CN}$  at  $120\text{ }^\circ\text{C}$  (a) directly after mixing and (b) after 30 min.

## Scheme 4. Tentative Mechanism for Formation of Intermediate Compound X



**Figure 9.** Mass region of the signal for the complex  $[(X)Cu(CH_3CN)]^+$  upon ESI sampling of the reaction mixture when conducted under (a) normal atmosphere or (b)  $Ar/^{18}O_2$ .



**Figure 10.** Branching ratios of the signals due to the reactant **1** and the product **2** as a function of reaction time in solution as monitored via ESI-MS with and without addition of **X** to the reaction mixture.

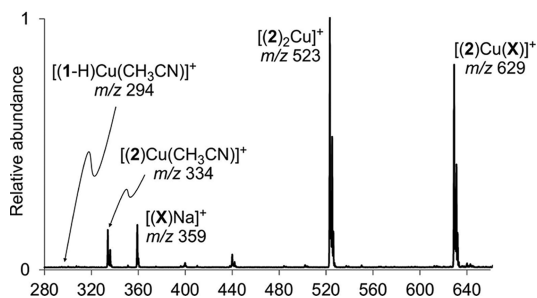


**Figure 11.** Positive-ion ESI mass spectrum for a 1:1:1 mixture of the reactant **1**, the product **2**, and compound **X** and 3 equiv of  $Cu(OAc)_2$  in  $CH_3CN$ .

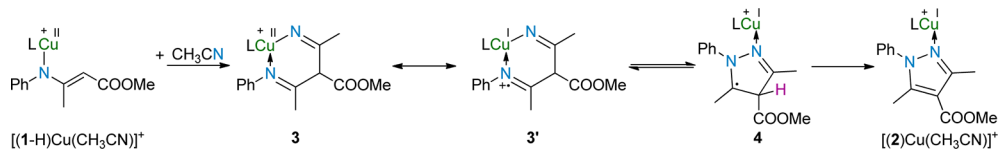
system is far from a 1:1:1 sampling of the equimolar mixture, but instead shows pronounced discrimination effects disfavoring the copper(II) complexes of the reactants over the copper(I) complexes of the product **2** as well as compound **X**. Relative binding of **1**, **2**, and **X** can be estimated as 1:200:100. The large preference of **2** in binding copper provides a quantitative explanation for the product inhibition of the title reaction proposed recently.<sup>23</sup>

**Mechanistic Implications for the Title Reaction.** The above experiments indicate that the title reaction commences with the deprotonation of the enaminone **1**, but with the exception of compound **X** the mass spectrometric experiments could not decipher other potential reaction intermediates. This leads to the obvious questions of why this is the case and hence also if ESI-MS is at all useful for such mechanistic studies of metal-mediated oxidation catalysis.

In order to address these questions, let us refer to a plausible route from **1** to **2** under copper catalysis (Scheme 5). From the reactant copper(II) complex  $[(1-H)Cu(CH_3CN)]^+$ , addition of acetonitrile can lead to C–C bond formation in intermediate **3**, which is connected with the putatively mesomeric form **3'**. Reduction from  $Cu^{II}$  to  $Cu^I$  can then trigger N–N bond formation (**3'** → **4**). In solution, the carbon-centered radical **4** is likely to be readily oxidized to product **2** via hydrogen-atom abstraction, and using ESI-MS we are able to observe directly only complexes of the product **2**. This is in agreement with the fact that the title reaction requires elevated temperatures and hence most probably is associated with high energy barriers. The equilibrium concentrations of putative intermediates are accordingly expected to be low. Nevertheless, the discovery and subsequent identification of compound **X** may well serve to demonstrate the additional insight ESI-MS can provide in mechanistic studies.

## CONCLUSIONS

The reaction mechanism of the intermolecular oxidative formation of pyrazole **2** via a C–C/N–N bond-formation cascade of the enaminone **1** is investigated systematically by means of electrospray-ionization mass spectrometry. The results show that the starting material, the enaminone **1**, first forms a complex with  $Cu(OAc)_2$  via exchange of one acetate ligand by the deprotonated substrate, i.e.,  $[1-H]$ . While no direct reaction intermediates are observed, the formation of an unexpected imidazolid-3-one derivative (compound **X**) is

Scheme 5. Suggested Pathway for the Reaction of  $[(1-H)Cu(CH_3CN)]^+$  to the Pyrazole Product

observed that involves an oxidative dimerization of **1** in the presence of dioxygen. A possible mechanism for the formation of **X** involves an initial oxidation in the  $\alpha$ -position of **1** followed by reaction with another equivalent of **1**, hydrolysis, and decarboxylation. Interestingly, addition of compound **X** to the reaction mixtures causes a moderate acceleration of the product formation.

## ■ ASSOCIATED CONTENT

### Supporting Information

Complete  $^1H$  and  $^{13}C$  NMR data for **X**. This information is available free of charge via the Internet at <http://pubs.acs.org>.

## ■ AUTHOR INFORMATION

### Corresponding Author

\*Phone: ++420 220 183 347. E-mail: [hyvl@uochb.cas.cz](mailto:hyvl@uochb.cas.cz).

### Notes

The authors declare no competing financial interest.

<sup>†</sup>Detlef Schröder passed away unexpectedly in August 2012.

## ■ ACKNOWLEDGMENTS

This work was supported by the Czech Academy of Sciences (RVO 61388963) and the European Research Council (AdG HORIZOMS). Our dear co-worker and mentor, Prof. Dr. habil. Detlef Schröder, suddenly passed away on August 22, 2012. The authors are very grateful for getting to know him, for his inspiring ideas and cheerful mentorship, and also for his writing a draft of the manuscript. The research work at WWU Münster was supported by the European Research Council under the European Community's Seventh Framework Program (FP7 2007–2013)/ERC Grant agreement no. 25936. Generous financial support by the International NRW Graduate School of Chemistry (M.S.) is gratefully acknowledged. The research of F.G. has been supported by the Alfried Krupp Prize for Young University Teachers of the Alfried Krupp von Bohlen und Halbach Foundation.

## ■ REFERENCES

- (1) (a) Ley, S. V.; Thomas, A. W. *Angew. Chem., Int. Ed.* **2003**, *42*, 5400. (b) Gwilhelm, E.; Blanchard, N.; Toumi, M. *Chem. Rev.* **2008**, *108*, 3054.
- (2) (a) Marko, I. E.; Giles, P. R.; Tsukazaki, M.; Brown, S. M.; Urch, C. J. *Science* **1996**, *274*, 2044. (b) Gamez, P.; Aibel, P. G.; Driessen, W. L.; Reedijk, J. *Chem. Soc. Rev.* **2001**, *30*, 376. (c) Punniyamurthy, T.; Rout, L. *Coord. Chem. Rev.* **2008**, *252*, 134. (d) Wendlandt, A. E.; Suess, A. M.; Stahl, S. S. *Angew. Chem., Int. Ed.* **2011**, *50*, 11062.
- (3) (a) Kitajima, N.; Moro-oka, Y. *Chem. Rev.* **1994**, *94*, 737–757. (b) Chaudhuri, P.; Hess, M.; Flörke, U.; Wieghardt, K. *Angew. Chem., Int. Ed.* **1998**, *37*, 2217. (c) Shearer, J.; Zhang, C. X.; Zakharov, L. N.; Rheingold, A. L.; Karlin, K. D. *J. Am. Chem. Soc.* **2005**, *127*, 5469.
- (4) Würtz, S.; Rakshit, S.; Neumann, J. J.; Dröge, T.; Glorius, F. *Angew. Chem., Int. Ed.* **2008**, *47*, 7230.
- (5) Neumann, J. J.; Suri, M.; Glorius, F. *Angew. Chem., Int. Ed.* **2010**, *49*, 7790.

(6) For a spectacular case in Pd/Cu catalysis in which DMF and additional ammonia lead to CN as a building block in C–H bond activation, see: Kim, J.; Chang, S. *J. Am. Chem. Soc.* **2010**, *132*, 10272.

(7) (a) Yamashita, M.; Fenn, J. B. *J. Phys. Chem.* **1984**, *88*, 4451. (b) Jayaweera, P.; Blades, A. T.; Ikononou, M. G.; Kebarle, P. *J. Am. Chem. Soc.* **1990**, *112*, 2452. (c) Fenn, J. B. *J. Am. Soc. Mass Spectrom.* **1993**, *4*, 524.

(8) Santos, L. S., Ed. *Reactive Intermediates: MS Investigations in Solution*; Wiley-VCH: Weinheim, Germany, 2010.

(9) (a) Chen, P. *Angew. Chem., Int. Ed.* **2003**, *42*, 2832. (b) Santos, L. S.; Knaack, L.; Metzger, J. O. *Int. J. Mass Spectrom.* **2005**, *246*, 84. (c) Santos, L. S. *Eur. J. Org. Chem.* **2008**, 235. (d) Müller, C. A.; Markert, C.; Teichert, A. M.; Pfaltz, A. *Chem. Commun.* **2009**, 1607. (e) Agrawal, D.; Schröder, D. *Organometallics* **2011**, *30*, 32.

(10) (a) Roithová, J.; Schröder, D. *Chem.—Eur. J.* **2008**, *14*, 2180. (b) Šrogl, J.; Hyvl, J.; Révész, A.; Schröder, D. *Chem. Commun.* **2009**, 3463. (c) Roithová, J.; Milko, P. *J. Am. Chem. Soc.* **2010**, *132*, 281. (d) Rokob, T. A.; Rulišek, L.; Šrogl, J.; Révész, Á.; Zins, E. L.; Schröder, D. *Inorg. Chem.* **2011**, *50*, 9968.

(11) Tintaru, A.; Roithová, J.; Schröder, D.; Charles, L.; Jušinski, I.; Glasovac, Z.; Eckert-Maksić, M. *J. Phys. Chem. A* **2008**, *112*, 12097.

(12) (a) Schröder, D.; Weiske, T.; Schwarz, H. *Int. J. Mass Spectrom.* **2002**, *219*, 729. (b) Trage, C.; Diefenbach, M.; Schröder, D.; Schwarz, H. *Chem.—Eur. J.* **2006**, *12*, 2454.

(13) Schröder, D. *Phys. Chem. Chem. Phys.* **2012**, *14*, 6382.

(14) Aggerholm, T.; Nanita, S. C.; Koch, K. J.; Cooks, R. G. *J. Mass Spectrom.* **2003**, *38*, 87.

(15) (a) Révész, Á.; Milko, P.; Žabka, J.; Schröder, D.; Roithová, J. *J. Mass Spectrom.* **2010**, *45*, 1246. (b) Zins, E. L.; Pepe, C.; Schröder, D. *J. Mass Spectrom.* **2010**, *45*, 1253.

(16) (a) Révész, Á.; Schröder, D.; Rokob, T. A.; Havlik, M.; Dolenský, B. *Angew. Chem., Int. Ed.* **2011**, *50*, 2401. (b) Schröder, D. *Collect. Czech. Chem. Commun.* **2011**, *76*, 351. (c) Severa, L.; Jirásek, M.; Švec, P.; Teplý, F.; Révész, Á.; Schröder, D.; Kašička, V.; Koval, D.; Císařová, I.; Šaman, D. *ChemPlusChem*, in press.

(17) (a) Hao, C.; March, R. E. *J. Mass Spectrom.* **2001**, *36*, 509. (b) Seymour, J. L.; Tureček, F. *J. Mass Spectrom.* **2002**, *37*, 533. (c) Schröder, D.; Holthausen, M. C.; Schwarz, H. *J. Phys. Chem. B* **2004**, *108*, 14407. (d) Milko, P.; Roithová, J.; Schröder, D.; Lemaire, J.; Schwarz, H.; Holthausen, M. C. *Chem.—Eur. J.* **2008**, *14*, 4318. (e) Tintaru, A.; Charles, L.; Milko, P.; Roithová, J.; Schröder, D. *J. Phys. Org. Chem.* **2009**, *22*, 229. (f) Tsierekzos, N. G.; Buchta, M.; Holý, P.; Schröder, D. *Rapid Commun. Mass Spectrom.* **2009**, *23*, 1550. (g) Ducháčková, L.; Roithová, J.; Milko, P.; Žabka, J.; Tsierekzos, N.; Schröder, D. *Inorg. Chem.* **2011**, *50*, 771. (h) Jaklová Dyrtrtová, J.; Jakl, M.; Schröder, D.; Čadková, E.; Komárek, M. *Rapid Commun. Mass Spectrom.* **2011**, *25*, 1037.

(18) See also: Tsybizova, A.; Tarábek, J.; Buchta, M.; Holý, P.; Schröder, D. *Rapid Commun. Mass Spectrom.* **2012**, *26*, 2287.

(19) Iyo, E. C.; Castleman, A. W.; Schröder, D.; Milko, P.; Roithová, J.; Ortega, J. M.; Cinellu, M. A.; Cocco, F.; Minghetti, G. *J. Am. Chem. Soc.* **2009**, *131*, 13009.

(20) The CID experiments at elevated energies were performed on a SYNAPT G2 mass spectrometer (also used for HR-MS), because the time scale of ion excitation in IT-MS is long compared to cooling collisions with the background helium, such that no really hard collisions can be realized.

(21) (a) Schade, M. A.; Fleckenstein, J. E.; Knochel, P.; Koszinowski, K. *J. Org. Chem.* **2010**, *75*, 6848. (b) Vikse, K. L.; Ahmadi, Z.; Manning, C. C.; Harrington, D. A.; McIndoe, J. S. *Angew. Chem., Int. Ed.* **2011**, *50*, 8304. (c) Vikse, K. L.; Ahmadi, Z.; Luo, J.; van der Wal,

N.; Daze, K.; Taylor, N.; McIndoe, J. S. *Int. J. Mass Spectrom.* **2012**, *323–324*, 8.

(22) Schröder, D. *Acc. Chem. Res.* **2012**, in press (doi: 10.1021/ar3000426).

(23) Suri, M.; Jousseume, T.; Neumann, J. J.; Glorius, F. *Green Chem.* **2012**, *14*, 2193.